J Therm Anal Calorim (2010) 99:229–235
DOI 10.1007/s10973-009-0088-2

Thermally formed oxide films on Al–6Zn–XMg ($X = 0$ and 2 mass%) alloys heated in different gases

Po-Chen Chen · Teng-Shih Shih · Juen-Shiou Chen

Received: 17 December 2008 / Accepted: 19 May 2009 / Published online: 28 August 2009

Abstract In this study, thermogravimetric analysis (TG) testing is used to measure the mass loss of polished Al–6Zn–XMg ($X = 0$ and 2 mass%) alloy samples heated at 773 K for 6 h in dry air or nitrogen gas. The progressive development of thermally formed oxides on an Al–6Zn–XMg ($X = 0$ and 2 mass%) alloy as shown by X-ray diffractometer analyses is discussed. Zn-spinel and Mg-spinel are detected on the Al–6Zn and Al–6Zn–2Mg alloy samples, respectively, and then heated in the dry air atmosphere; AlN and Mg_3N_2 are detected in alloy samples heated in nitrogen gas. The chain reactions that cause the serrated change in the mass loss curve are proposed and discussed.

Keywords AlN · Mg_3N_2 · Spinel · TG · XRD

Introduction

When aluminum is heated in air to temperatures above 723 K, an air-formed oxide film develops on its surface. Initially, an amorphous oxide film is formed, but subsequently, γ-alumina crystals develop at the metal–oxide interface [1–4]. Shih et al. performed thermogravimetric analysis (TG) and X-ray powder diffractometer analysis on pure aluminum samples that had been heated in air from room temperature up to 883 K. They observed an apparent mass gain at 832 K, which occurred due to the transformation of gibbsite to diaspore. Such thermally formed oxide films are composed of complex oxides such as gibbsite, diaspore, α-Al_2O_3, and γ-Al_2O_3 [5].

When Al–Mg powders are sintered, nano-sized crystalline precipitates tend to form in the interface [6]. These precipitates could be $MgAl_2O_4$ or MgO depending on the sintering temperature and Mg content. Spinel has been observed only when the Mg content is less than 2.5% [7, 8]. The magnesium reduced the surface oxide film on aluminum metal by the following reaction: $3Mg + 4Al_2O_3 \rightarrow 3MgAl_2O_4 + 2Al$ or $3Mg + Al_2O_3 \rightarrow 3MgO + 2Al$. When the Mg level is high, MgO rather than $MgAl_2O_4$ products dominate and are present within the thermally formed oxide film [8].

Nitrogen is commonly used for degassing during the melting of aluminum alloys. Nitrogen gas interacts with the aluminum to form AlN in the melt [9, 10]. Direct melt oxidation has become an attractive process for the fabrication of ceramic matrix composites such as Al_2O_3/Al and AlN/Al. The interaction between the nitrogen gas and the aluminum alloy melt and the method of fabricating the AlN metal matrix composites are quite important. Hanabe et al. grew Al_2O_3/Al composite from Al–Zn–XMg alloys ($X =$ 0–0.36 wt%) [11]. Composites formed as a result of cyclic formation and reduction in molten aluminum of ZnO. ($X = 0$–0.36 wt%) [11]. Composite formed as a result of the cyclic formation and reduction in molten aluminum of ZnO.

High-strength aluminum alloys containing 4–6 mass% Zn and 1–3 mass% Mg, such as AA7005 and 7075, are widely used in industry. The study of thermal oxidation can provide basic knowledge for understanding the oxide formed from the processes of recycling and/or melting Al–Mg–Zn alloys. We take steps toward an understanding of the kinetic reaction of Al–6Zn–XMg ($X = 0$ and 2 mass%) alloy oxidation in this study.

P.-C. Chen · T.-S. Shih (✉) · J.-S. Chen
Department of Mechanical Engineering, National Central University, Chung-Li 32001, Taiwan, ROC
e-mail: t330001@cc.ncu.edu.tw

Experimental procedure

The Al–6Zn–XMg ($X = 0$ and 2 mass%) alloy cakes used for our experiments (supplied by HYDRO Inc.) were first solution-treated at 743 K for 6 h and then quenched in water. After solution treatment, samples were polished for optical micrograph observation. The grain size was about 300–400 μm. An EMGA-521 hydrogen analyzer (HORIBA, Ltd.) was used to test the hydrogen content of the alloy samples. The hydrogen content for the solution-treated Al–6Zn–XMg (X = 0 and 2 mass%) alloy sample was 0.5 and 0.89 cm^3/100 g, respectively.

The alloy cakes were machined into the desired sizes: 10 × 10 × 5 mm^3 cubes for scanning electron microscope (SEM) and electron probe micro-analyzer (EPMA) analyses; 10 × 6 × 1 mm^3 for X-ray diffraction (XRD) and electron spectroscopy for chemical analysis (ESCA) testing; and 6 mm (diameter) × 1 mm for TG analysis testing. All surfaces of the samples were dry polished with SiC paper with grit sizes ranging from P400 to P2000. Thermogravimetric analysis with a Perkin Elmer TG-7 was carried out to record the mass variations in the samples heated in dry air or nitrogen gas. The flow rate was 49.8 mL/min, and the heating rate was 8.3 K/min; the sample was maintained for 6 h at 773 K.

For the other test, the alloy samples were set in a quartz tube (volume 2100 cm^3) and subjected to a resistant heating at 773 K for different time spans. In cases where a nitrogen atmosphere was used, the air was pumped out of the chamber and then filled with pure commercial N_2 gas. After being heated for a specific time span, the alloy samples were removed from the furnace and cooled to room temperature. The thermally treated samples coded with sample "A"–"D" were then subjected to X-ray diffractometer testing. A glancing incident angle X-ray powder diffractometer was used to test the constituents of the surface oxide film. A copper target was used in the test; the wavelength and theta angle were determined to be 0.154 nm and 1°, respectively.

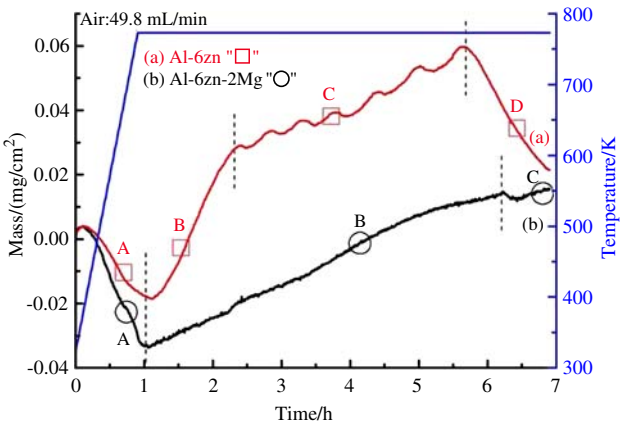

Fig. 1 Thermogravimetric analysis results of the Al–6Zn–XMg ($X = 0$ and 2 mass%) sample heated at 773 K in dry air; heating rate = 8.3 K/min; air flow rate = 49.8 mL/min

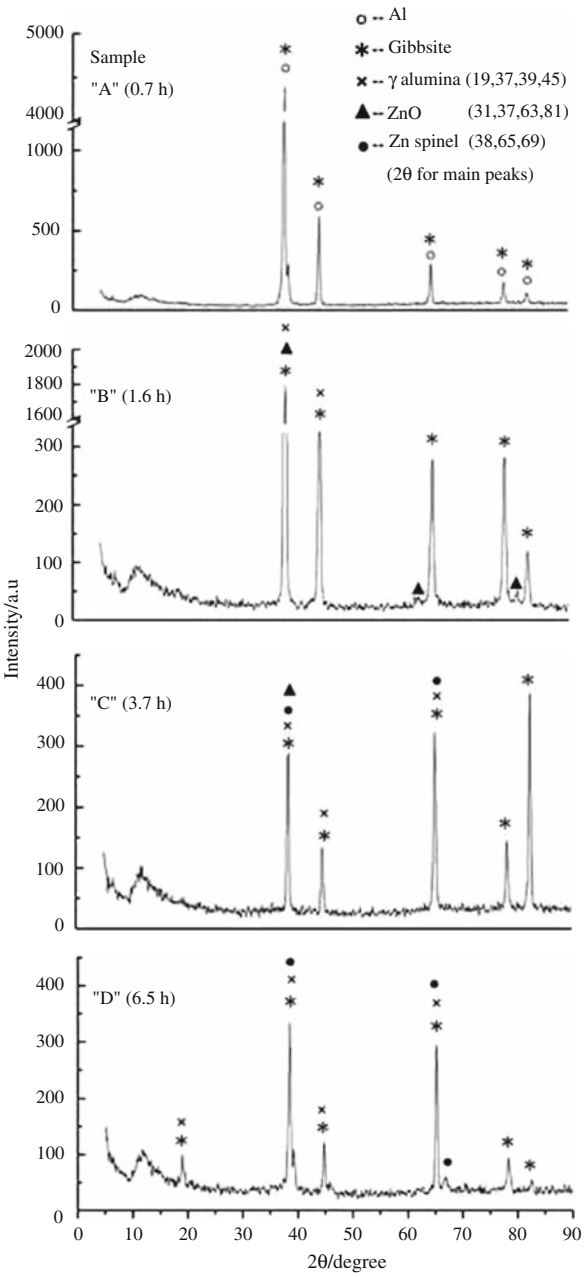

Fig. 2 X-ray diffractometer analysis results (intensity versus 2θ angle) of the thermally formed oxide film on the Al–6Zn alloy sample heated at 773 K for samples "A" (0.7 h), "B" (1.6 h), "C" (3.7 h), and "D" (6.5 h)

Cross sections of the samples were polished using alumina powder (0.3 microns). Colloidal silica was then used for further polishing. A conductive copper plating layer was coated on the oxide film prior to SEM observation. The composition of the oxide film on the surface was analyzed by Auger electron spectroscopy.

Results and discussion

Formation of a surface oxide film in the presence of dry air

Figure 1 shows the TG analysis test results for the Al–6Zn–XMg ($X = 0$ and 2 mass%) alloy samples heated in dry air. The temperature curves (maintained at 773 K) are also included. Gibbsite ($2Al + 6H_2O \rightarrow 2Al(OH)_3 + 3H_2$) was formed when aluminum was subjected to heating temperatures of 300–400 K [12]. During heating, the Al–6Zn alloy sample hydrated to form gibbsite first. This increased the mass of the samples ($Al(OH)_3 = 77.980$ g/mol) slightly (see Fig. 1 curve (a)). As the temperature increased, gibbsite was transformed first to boehmite ($AlO(OH) = 59.989$ g/mol) by to the reaction $Al(OH)_3 \rightarrow AlO(OH) + H_2O$, and then to γ-alumina (101.960 g/mol) by the reaction $2AlO(OH) \rightarrow Al_2O_3 + H_2O$. The dehydration reactions decreased the mass of the samples (see sample "A" in Fig. 2 and Fig. 1 curve (a)).

Dehydration was likely to be complete after a holding time of 1 h (see Fig. 1). Gamma alumina could be expected to form on the top layer of the oxide film and to increase in intensity following an extended heating time (1.6 h) (see sample "B" in Fig. 2). With an increase in the heating (holding) time, the Zn accumulates at the interface between the substrate and the oxide film. This Zn would then diffuse into the oxide film to react with oxygen and to form ZnO (81.370 g/mol) locally after the reaction of Al with oxygen. Formation of ZnO and/or γ-alumina increased the sample mass as shown in sample "B" in Fig. 2, and Fig. 1 curve (a). The constituents of the thermally formed oxide films on sample "B" mainly include γ-alumina, gibbsite, and some ZnO.

ZnO was formed after the completion of dehydration. The sample then experienced the following reactions: $4ZnO + 2Al \rightarrow ZnAl_2O_4 + 3Zn$ ($\Delta G_f = -638.66$ kJ/mol at 773 K), and concurrently $3ZnO + 2Al \rightarrow Al_2O_3 + 3Zn$ ($\Delta G_f = -598.76$ kJ/mol at 773 K), and $3ZnAl_2O_4 + 2Al \rightarrow 4Al_2O_3 + 3Zn$ ($\Delta G_f = -479.06$ kJ/mol at 773 K); see Table 1. All these reactions acted to convert the ZnO into

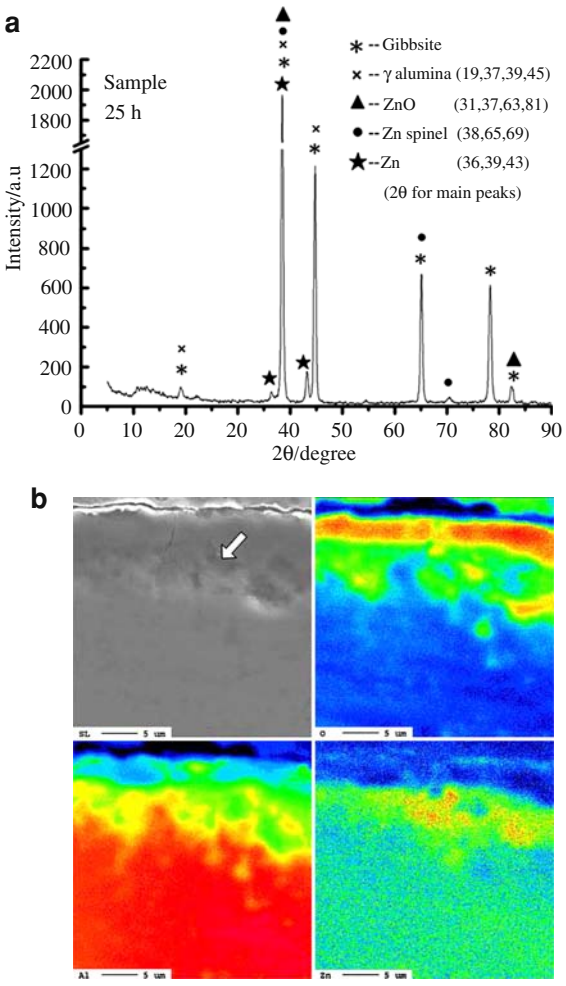

Fig. 3 **a** X-ray diffractometer analysis results of the thermally formed oxide film on the Al–6Zn alloy samples heated at 773 K for 25 h; **b** EPMA images showing a sectional view, including the oxide film and substrate, associated with the Al, O, and Zn mapping

Table 1 The prospective reactions occurred at 773 K for Al–6Zn–XMg ($X = 0$ and 2 mass%) alloys heated in air and in nitrogen gas; activation energies and enthalpies are also included

Atmosphere	Average E_a/kJ mol^{-1}	Reactions	Gibb's free energy kJ mol^{-1} (773 K)	Enthalpy kJ mol^{-1} (773 K)
Air Al–6Zn	75	$4ZnO + 2Al \rightarrow ZnAl_2O_4 + 3Zn$	−638.66	−592.35
		$3ZnO + 2Al \rightarrow Al_2O_3 + 3Zn$	−598.76	−584.95
		$3ZnAl_2O_4 + 2Al \rightarrow 4Al_2O_3 + 3Zn$	−479.06	−562.73
Air Al–6Zn–2Mg	135	$4Al_2O_3 + 3Mg \rightarrow 3MgAl_2O_4 + 2Al$	−261.84	−281.12
		$MgO + Al_2O_3 \rightarrow MgAl_2O_4$	−41.73	−44.30
N_2 Al–6Zn	80	$2Al + N_2 \rightarrow 2AlN$	−473.34	−637.49
		$4AlN + 3O_2 \rightarrow 2Al_2O_3 + 2N_2$	−1886.808	−2030.38
N_2 Al–6Zn–2Mg	138	$3Mg + N_2 \rightarrow Mg_3N_2$	−304.617	−460.74
		$Mg_3N_2 + 2Al \rightarrow 2AlN + 3Mg$	−168.723	−176.75

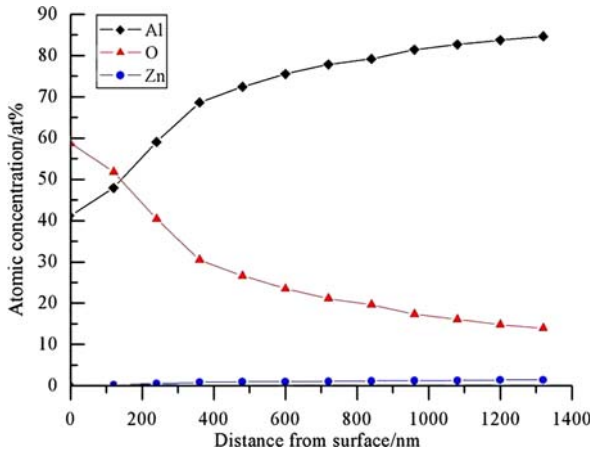

Fig. 4 ESCA analysis results showing the measured atomic concentrations of Al, O, and Zn as a function of distance from the surface (computed from the sputtering time) for Al–6Zn alloy samples heated at 773 K for 25 h

alumina, which greatly decreased the intensity of ZnO, as shown in the test results of sample "C" (see Fig. 2). The oxide film on sample "C" was therefore composed of Zn-spinel, γ-alumina, and gibbsite.

Increasing the heating time to 6.5 h significantly increased the amount of $ZnAl_2O_4$ and/or Al_2O_3 (see sample "D" in Fig. 2). $ZnAl_2O_4$ possesses a greater molar volume than alumina: 42.639 vs. 25.175 cm^3/mol [13]. After a certain amount of $ZnAl_2O_4$ (183.35 g/mol) is transformed to Al_2O_3, voids would form within the oxide film. With the existence of voids, Zn would possibly evaporate from the substrate, resulting in a continuous reduction in the mass of the sample (see Fig. 1 curve (a) of the mass loss curve).

Increasing the heating time to 25 h increased the intensities of Al_2O_3 and metallic Zn that reacted (see Fig. 3a). The mapping of O, Al, and Zn on this alloy sample clearly indicate that the γ-alumina is located primarily at the top layer and near the interface, as shown in Fig. 3b. Voids could be initiated from the interior of the film to open up the top layer to form a crack. Figure 4 shows the results of ESCA analysis and confirms that the top layer is indeed gamma alumina. The concentration of Zn (from $ZnAl_2O_4$ and/or metallic Zn) increases with the distance from the top surface.

The mass loss of the heated Al–6Zn–2Mg alloy sample is also included in Fig. 1 curve (b). Gamma alumina persistently formed in the film via the dehydration of gibbsite. The Mg at the interface increased concurrently. This Mg then diffused to react with the γ-alumina and to form $MgAl_2O_4$: $4Al_2O_3 + 3Mg \rightarrow 3MgAl_2O_4 + 2Al$ ($\Delta G_f = -261.84$ kJ/mol at 773 K); see Table 1. This reaction increased the mass of the $MgAl_2O_4$ sample (142.270 g/mol). It was also possible for the periclase (MgO = 40.310 g/mol) to react with the γ-alumina to form $MgAl_2O_4$: $MgO + Al_2O_3 \rightarrow MgAl_2O_4$ ($\Delta G_f = -41.73$ kJ/mol at 773 K); see Table 1. The alumina existing in the thermally formed oxide film was likely covered by (or contacted with)

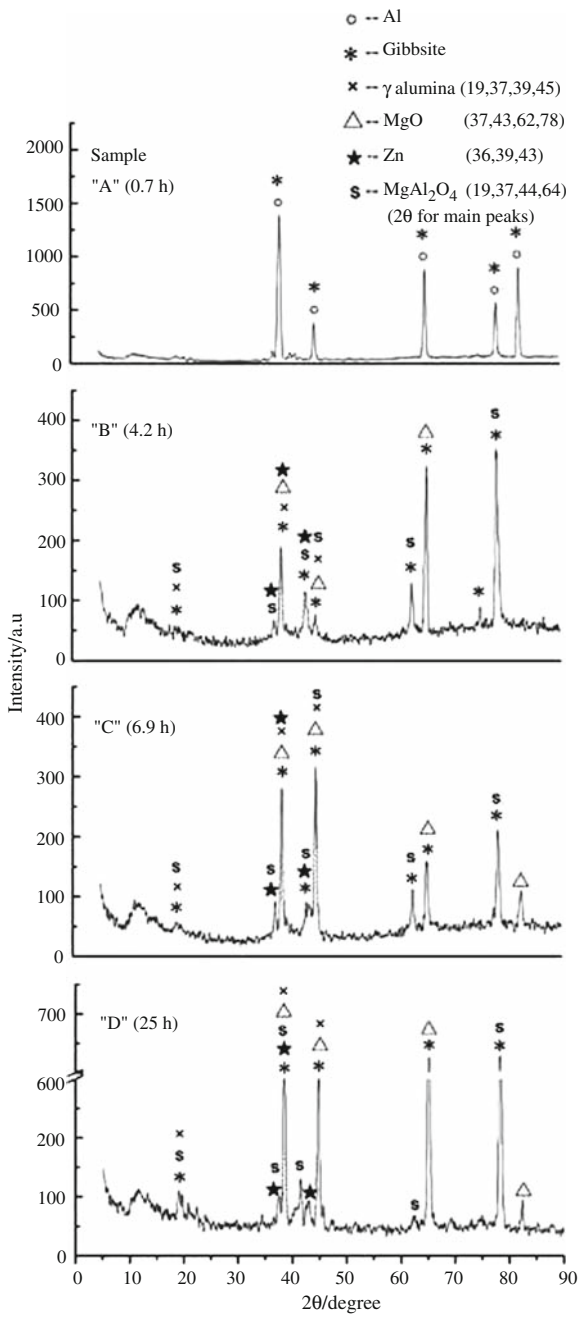

Fig. 5 **a** X-ray diffractometer analysis results (intensity versus 2θ angle) of the thermally formed oxide on the Al–6Zn–2Mg alloy sample heated at 773 K for samples "A" (0.7 h), "B" (4.2 h), "C" (6.9 h), and "D" (25 h); **b** sectional view of the thermally formed oxide film on the Al–6Zn–2Mg alloy samples heated at 773 K for 25 h; EPMA images of the Al, O, Mg, and Zn mapping are included

MgO and/or transformed to $MgAl_2O_4$ [8]. This is why no Zn-spinel, only $MgAl_2O_4$, was detected in sample "B" (Fig. 5a), which was composed of MgO, $MgAl_2O_4$, and γ-alumina, accompanied by some gibbsite.

As the heating time was increased to 6.9 h, the intensities of the $MgAl_2O_4$ and metallic zinc concentration increased, as indicated by the X-ray diffractometer results of sample "C"

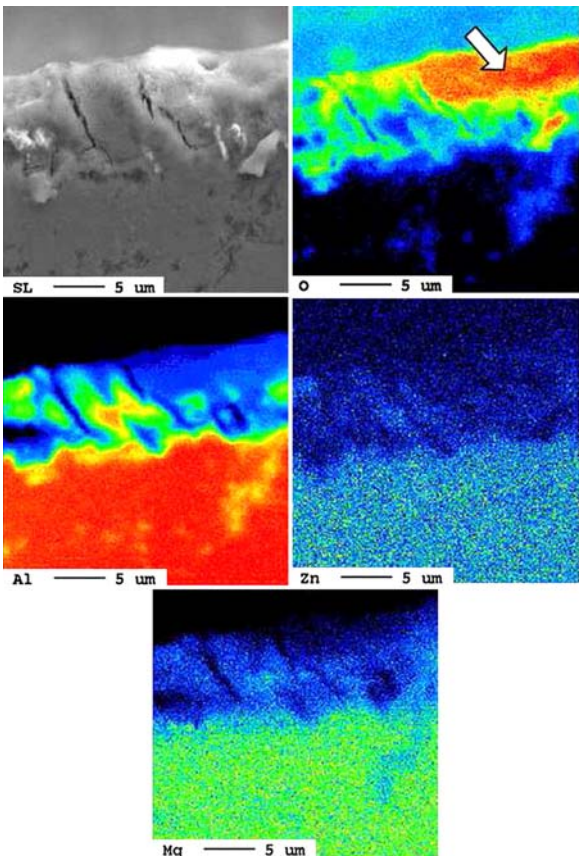

Fig. 5 continued

(Fig. 5a). When the heating (holding) time was extended, the intensities of the MgO and $MgAl_2O_4$ concentrations increased, as indicated by the X-ray diffractometer results of sample "D" (Fig. 5a). The $MgAl_2O_4$ product (39.085 cm^3/mol) was greater in molar volume than the reacting Al_2O_3 (25.175 cm^3/mol) and MgO (10.661 cm^3/mol). The reaction $MgO + Al_2O_3 \rightarrow MgAl_2O_4$ generates stress that cracks the oxide film, as shown in Fig. 5b. The analyses of O, Al, and Mg mapping indicate that areas rich in oxygen likely existed with γ-alumina (as indicated by the arrow), and $MgAl_2O_4$ was located nearby. Zn was distributed over the oxide film, but it was less concentrated in the region occupied by the γ-alumina. In Fig. 6, it can be seen that the top layer of thermally formed oxide film is rich in MgO and $MgAl_2O_4$. Gamma alumina that formed in the early stage of heating (dehydration product and located at the top layer) was mostly converted to $MgAl_2O_4$. From Fig. 5b, we can observe that γ-alumina colonies became less plentiful while the amount of the nearby $MgAl_2O_4$ grew.

The hydrogen contents of the solution-treated Al–6Zn–XMg ($X = 0$ and 2 mass%) alloy samples were 0.5 and 0.89 cm^3/100 g of Al, respectively. Increasing Mg content in the alloy increases the hydrogen content absorbed in the sample. After heating to 773 K for 6 h, the hydrogen

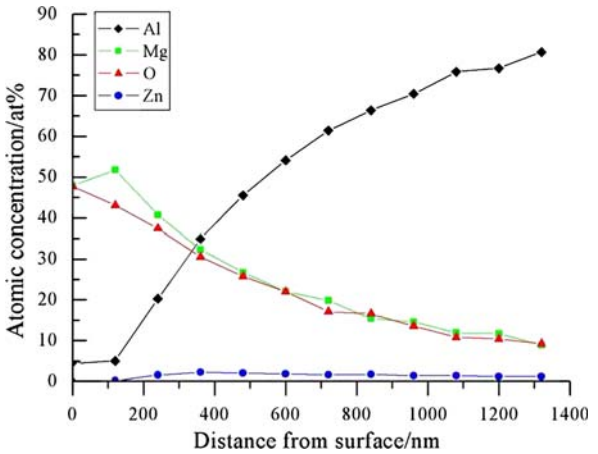

Fig. 6 ESCA analysis results showing the measured atomic concentrations of Mg, Al, O, and Zn as a function of distance from the surface (computed from the sputtering time) for Al–6Zn–2Mg alloy samples heated at 773 K for 25 h

content of the alloy samples decreased to 0.084 and 0.097 cm^3/100 g of Al, respectively. The heating process significantly decreases the hydrogen content of the alloy samples. Hydrogen diffused from the substrate and moved toward the interface between the film and the substrate to react with oxygen in the film, thereby persistently forming gibbsite during the heating and cooling process.

Formation of a surface oxide film in a nitrogen atmosphere

Figure 7 shows the TG analysis test results of the Al–6Zn–XMg ($X = 0$ and 2 mass%) alloy samples after being heated in a nitrogen gas atmosphere. The mass loss curve is similar to that obtained from samples heated in dry air (compare Fig. 7 with Fig. 1). Commercial nitrogen gas contains some oxygen [10], and the Al–6Zn–XMg ($X = 0$ and 2 mass%)

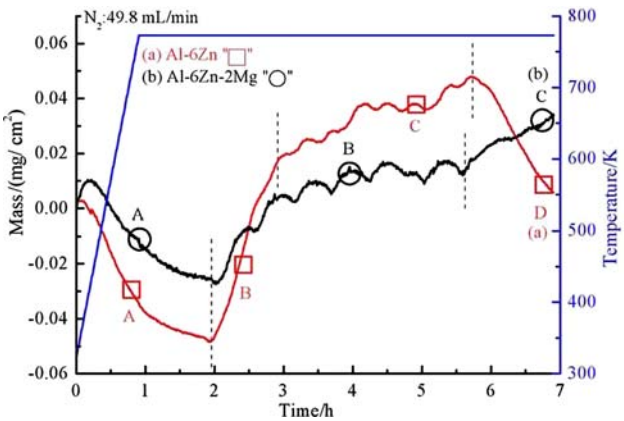

Fig. 7 Thermogravimetric analysis results of the Al–6Zn–XMg ($X = 0$ and 2 mass%) alloy samples heated at 773 K in a nitrogen gas atmosphere; heating rate = 8.3 K/min; air flow rate = 49.8 mL/min

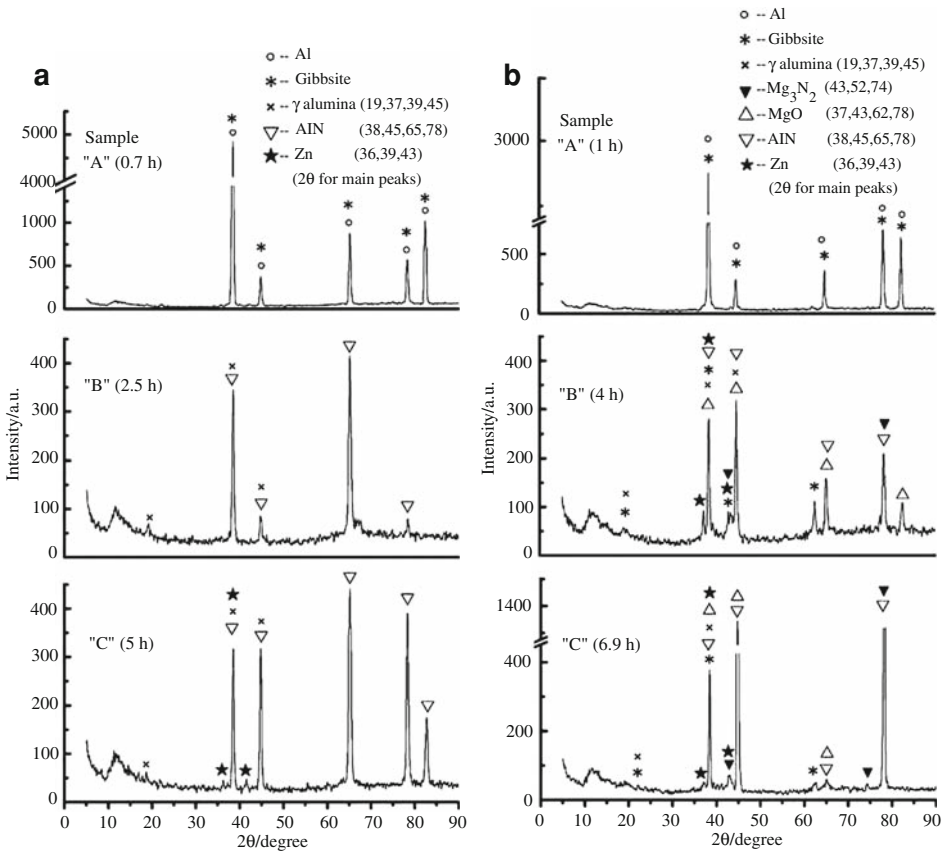

Fig. 8 **a** X-ray diffractometer analysis results (intensity versus 2θ angle) for Al–6Zn alloy samples heated at 773 K in a nitrogen gas atmosphere for samples "A" (0.7 h), "B" (2.5 h), and "C" (5 h). **b** X-ray diffractometer analysis results (intensity versus 2θ angle) for the Al–6Zn–2Mg alloy samples heated at 773 K in a nitrogen gas atmosphere for samples "A" (1 h), "B" (4.0 h), and "C" (6.9 h)

alloy samples themselves contain some amounts of hydrogen. For heating the Al–6Zn alloy sample in a nitrogen gas atmosphere, gibbsite was produced first and then dehydrated, leading to a loss in sample mass (see Fig. 7 curve (a)). Zheng et al. described the adsorption of N_2–O_2 pairs at the surface of an Al melt. Intermediate physisorption is involved in the chemisorptions of N_2 gas. N_2 gas cannot be chemisorbed when oxygen impurities in the N_2 atmosphere exceed a threshold limit ($\sim$100 ppm), which means that significant AlN cannot be formed [10]. Dehydration is completed after about 2 h and it consumes most of the oxygen available in the film. The aluminum then reacts with nitrogen to form AlN by following reaction: $2Al + N_2 \rightarrow 2AlN$ ($\Delta G_f = -473.34$ kJ/mol at 773 K and AlN = 40.990 g/mol; see Table 1) to increase sample mass significantly (see Fig. 7 and the XRD analysis in Fig. 8a of sample "B").

After the heating time increased to 5 h, the surrounding atmosphere persistently offered limited amounts of oxygen to convert the AlN to Al_2O_3 and significantly increased the sample mass; $4AlN + 3O_2 \rightarrow 2Al_2O_3 + 2N_2$ ($\Delta G_f = -1886.808$ kJ/mol at 773 K and Al_2O_3 = 101.960 g/mol; see Table 1). XRD analysis shows the AlN phases, γ-alumina, and some metallic Zn in the thermally formed oxide films of sample "C" (see Fig. 8a).

For heating the Al–6Zn–2Mg alloy sample in a nitrogen gas atmosphere, dehydration of gibbsite is also likely to be complete after about 2 h (see Fig. 7 curve (b)). XRD analysis shows that the thermally formed oxide films are composed of the phases of Mg_3N_2, MgO, AlN, metallic Zn, and some γ-alumina (see Fig. 8b, sample "B"). Magnesium diffused from the substrate into the film to react with the limited oxygen in the film to carry out the reaction $2Mg + O_2 \rightarrow 2MgO$. After the oxygen was consumed in the film, aluminum and magnesium would react with the nitrogen to form AlN and Mg_3N_2: $2Al + N_2 \rightarrow 2AlN$ ($\Delta G_f = -473.34$ kJ/mol at 773 K) and $3Mg + N_2 \rightarrow Mg_3N_2$ ($\Delta G_f = -304.617$ kJ/mol at 773 K); see Table 1. The molar weights of AlN and Mg_3N_2 were 40.988 and 100.949 g/mol, respectively. The formation of AlN and Mg_3N_2 could increase the sample mass significantly, as shown in Fig. 7.

Aluminum persistently offered from the substrate to react with the Mg_3N_2 to produce AlN: $Mg_3N_2 + 2Al \rightarrow 2AlN + 3Mg$ ($\Delta G_f = -168.723$ kJ/mol at 773 K). Increasing the heating time to 6.9 h significantly increased the intensity of AlN, as shown in the sample "C" curve in Fig. 8b. Producing Mg_3N_2 could significantly increase the mass of the alloy samples. However, the transformation of 1 M Mg_3N_2 to 2 M AlN would lead to a reduction in the mass of the samples. The concurrent occurrence of the above reactions to produce Mg_3N_2 and converting to AlN led to the serrated shape of the mass loss curve. Activation

energies for different reactions in air atmosphere and nitrogen gas were also calculated and compared as listed in Table 1 [14].

Conclusions

The thermally formed oxide film on an Al–6Zn alloy sample heated in a dry air atmosphere was composed of $ZnAl_2O_4$, γ-alumina, and metallic Zn associated with some gibbsite; the film on the Al–6Zn–2 mass% Mg alloy sample consisted of $MgAl_2O_4$, MgO, γ-alumina, metallic Zn, and gibbsite. The thermally formed surface oxide films on the Al–6Zn–(0 and 2 mass%) Mg alloy samples heated in nitrogen gas atmosphere were loose in structure and had cracks. The Al–6Zn sample was mainly composed of AlN, γ-alumina, metallic Zn, and gibbsite. The Al–6Zn–2 mass% Mg sample had complex oxides of MgO, Mg_3N_2, AlN, and γ-alumina, along with a little metallic Zn.

Acknowledgements The authors would like to thank the National Science Council of Taiwan for providing financial support for this study under Grant Number NSC97-2221-E-008-017.

References

1. Doherty PF, Davis RS. Direct observation of the oxidation of aluminum single-crystal surfaces. J Appl Phys. 1963;34:619–28.
2. Beck AF, Heine MA, Caule EJ, Pryor MJ. The kinetics of the oxidation of Al in oxygen at high temperature. Corrosion Sci. 1967; 7:1–22.
3. Dignam MJ, Faucett WR, Böhni H. The kinetics and mechanism of oxidation of superpurity aluminum in dry oxygen. J Electrochem Soc. 1966;113:656–62.
4. Eldridge JI, Hussey RJ, Mitchell DF, Graham MJ. Thermal oxidation of single-crystal aluminum at 550°C. Oxid Met. 1988;30: 301–28.
5. Shih TS, Liu ZB. Thermally-formed oxide on aluminum and magnesium. Mater Trans. 2006;475:1347–53.
6. Xie G, Ohashi O, Song M, Mitsuishi K, Furuya K. Reduction mechanism of surface oxide films and characterization of formations on pulse electric-current sintered Al–Mg alloy powders. Appl Surf Sci. 2005;241:102–6.
7. Kim DH, Yoon EP, Kim JS. Oxidation of an aluminum −0.4 wt% magnesium alloy. J Mater Sci Lett. 1996;15:1429–31.
8. Scamans GM, Butler EP. In situ observations of crystalline oxide formation during aluminum and aluminum alloy oxidation. Metallurg Mater Trans A. 1975;6:2055–63.
9. Hou Q, Mutharasan R, Koczak M. Feasibility of aluminium nitride formation in aluminum alloys. Mater Sci Eng A. 1995;195:121–9.
10. Zheng Q, Reddy RG. Mechanism of in situ formation of AlN in Al melt using nitrogen gas. J Mater Sci. 2004;39:141–9.
11. Hanabe M, Jayaram V, Bhaskaran TA. Growth of Al, O,/Al composites from Al-Zn alloys. Acta Metallurgica et Materialia. 1996; 40:819–29.
12. Santos PS, Santos HS, Toledo SP. Standard transition aluminas electron microscopy studies. J Mater Res. 2000;3:104–14.
13. Roberts WL, Campbell TJ, Rapp GR Jr, Wilson WE. Encyclopedia of minerals. 2nd ed. New York: Van Nostrand Reinhold Company; 1990.
14. Burnham AK, Dinh LN. A comparison of isoconversional and model-fitting approaches to kinetic parameter estimation and application predictions. J Thermal Anal. 2007;89:479–90.